# Nanothermite reactions: Is gas phase oxygen generation from the oxygen carrier an essential prerequisite to ignition?

Guoqiang Jian, Snehaunshu Chowdhury, Kyle Sullivan [1], Michael R. Zachariah *

*Department of Mechanical Engineering, University of Maryland, College Park, MD 20742, USA*
*Department of Chemistry and Biochemistry, University of Maryland, College Park, MD 20742, USA*

ABSTRACT

In this study we investigate the role of gas phase oxygen on ignition of nanothermite reactions. By separately evaluating the temperature at which ten oxidizers release gas phase species, and the temperature of ignition in an aluminum based thermite, we found that ignition occurred prior to, after or simultaneous to the release of gas phase oxygen depending on the oxidizer. For some nanothermites formulations, we indeed saw a correlation of oxygen release and ignition temperatures. However, when combined with in situ high heating stage microscopy indicating reaction in the absence of $O_2$, we conclude that the presence of free molecular oxygen cannot be a prerequisite to initiation for many other nanothermites. This implies that for some systems initiation likely results from direct interfacial contact between fuel and oxidizer, leading to condensed state mobility of reactive species. Initiation of these nanothermite reactions is postulated to occur via reactive sintering, where sintering of the particles can commence at the Tammann temperature which is half the melting temperature of the oxidizers. These results do not imply that gas phase oxygen is unimportant when full combustion commences.

© 2012 Published by Elsevier Inc. on behalf of The Combustion Institute.

## 1. Introduction

Metal–oxidizer mixtures have recently generated considerable interest in the combustion community due to their high energy density on a mass/volumetric basis as compared to traditional organic compounds [1]. When both the metal and the oxidizer comprises of nanoparticles, such mixtures are called nanothermites or metastable interstitial/intermolecular composites (MICs). By using nanoparticles, the fuel and oxidizer can be finely intermixed, thus improving the interfacial contact and greatly reducing the characteristic mass diffusion length between the reactants resulting in enhanced reactivity of the nanothermites as evident from higher flame speeds [2] and lesser ignition delay reported in literature [3].

While fuels like boron [4] and silicon [5] have been explored, nano-aluminum (n-Al) is predominantly the fuel of choice due to a combination of its high energy density, reactivity, low cost, and nontoxic nature. A variety of oxidizers have been studied, and the choice often depends on the particular application. Copper oxide (CuO) [6,7], iron oxide ($Fe_2O_3$) [6], molybdenum oxide ($MoO_3$) [2,8–13], tungsten oxide ($WO_3$) [11] and bismuth oxide ($Bi_2O_3$) [11,14] are the commonly used oxidizers in nanothermites.

Nano-aluminum particles typically have a thin ($\sim$2–5 nm in thickness) amorphous aluminum oxide shell surrounding the elemental core of aluminum, protecting the particle from further oxidation in air. These particles are typically aggregates of spherical primary particles, although recent work has shown the formation of single domain aluminum crystals [15]. For nanoparticles, the oxide shell can represent a significant portion of the particle mass. Oxidizer particles used in prior studies, on the other hand, display various morphologies. They have been used in the form of platelets [11,13], crystalline sheets [11], spheres [6,14] and nanorods [11,14,16].

An interesting and unresolved question in the study of nanothermites is the way they ignite/react depending on the heating rates involved. At lower heating rates ($\sim$1–20 K/min), Trunov et al. [17] has shown the oxide shell to undergo phase transformations making it permeable to the mass transport of aluminum and oxygen across the shell. Since reaction was observed to occur below the melting temperature of bulk aluminum (933 K), the authors suggested that outward diffusion of Al dominates when the oxide is amorphous while inward diffusion of oxygen dominates for crystalline alumina. At faster heating rates ($\sim$10$^3$ K/s), Rai et al. [18] showed the formation of hollow aluminum particles after oxidation. They argued that the aluminum in the core must have leaked out by diffusion due to concentration and/or pressure gradient across the shell. Similar experimental evidence have also been

* Corresponding author at: Department of Mechanical Engineering and Department of Chemistry and Biochemistry, University of Maryland, College Park, MD 20742, USA. Fax: +1 301 314 9477.
   *E-mail address:* mrz@umd.edu (M.R. Zachariah).
[1] Present address: Lawrence Livermore National Laboratory, Livermore, CA 94551, USA.

demonstrated by Nakamura et al. [19]. Pursuing this idea, we have shown in a previous work [20] that diffusion of reactive species is controlling even at heating rates on the order of $10^5$ K/s. Based on the observed ignition delay, an effective diffusion rate of $\sim10^{-10}$ cm$^2$/s was calculated. In another recent study by our group, Sullivan et al. [21] used a specially-designed heating holder to heat n-Al at $10^6$ K/s inside a scanning electron microscope. In this particular study, a significant heating pulse (300–1473 K at $\sim10^6$ K/s, and then held at 1473 K for 10 ms) was necessary before shell breakdown occurred, and outwards migration of Al could visually be identified. A smaller heating pulse, although above the melting temperature of Al, induced no changes within the very fast heating and cooling timescale of this experimental technique. Using Al–WO$_3$ nanothermite mixture, the authors suggested a condensed phase initiation/reaction. At even higher heating rates ($\sim10^7$–$10^8$ K/s) Levitas et al. [22] proposed the "Melt Dispersion Mechanism (MDM)" in which the aluminum core melts and exerts mechanical stress on the solid oxide shell. This causes spallation of the shell, and is predicted to happen at or near the melting temperature of aluminum, viz. 933 K. The violent rupture of the shell causes tensile stress on the molten Al core, thus unloading small molten clusters of aluminum at high velocities. The reaction rate in this mechanism is inherently not rate-limited by the diffusion of oxidizer/fuel through the shell. In separate studies using time resolved mass spectrometry of rapidly heated ($\sim10^5$ K/s) nano-aluminum and nanothermites [23,24], no evidence of aluminum clusters were found but only elemental aluminum was detected. Based on these previous works and the lack of aluminum clusters being detected, our current speculation is that aluminum migrates through its shell via a diffusion mechanism.

The correlation between oxygen release and nanothermite reaction have been suggested by Schoenitz et al. [12]. They conducted thermal analysis at low heating rates on Al–MoO$_3$ nanothermites and tentatively concluded that the appearance of the first exothermic peak at $\sim$470 K is indicative of the decomposition of MoO$_3$ into MoO$_2$ and oxygen (O). The authors commented that the in situ oxygen produced due to decomposition of the oxidizer could readily escape if the nanothermite mixture is prepared from the individual components in powder form. Similar suggestions of the possible decomposition of the oxidizer have been put forth to explain the kinetic behavior for Al–CuO nanothermite reactions observed under low heating rates by Umbrajkar et al. [7]. Direct experimental evidence of oxygen release from the oxidizer and its correlation to the ignition of nanothermites was first shown by Zhou et al. [23] using a T-Jump time of flight mass spectrometer (T-Jump TOFMS). Details of the operation of this instrument is available in a previous publication [25]. In short, the nanothermites were ignited on a platinum wire by heating them by an electrical pulse ($\sim10^5$ K/s) and the species produced during the reaction were sampled every 100 µs. With a high heating rate ($\sim5 \times 10^5$ K/s) we detected the release of molecular oxygen (O$_2$) from CuO and Fe$_2$O$_3$ in the reaction of Al–CuO and Al–Fe$_2$O$_3$ thermites. The liberated O$_2$ was one of the first species to be detected temporally thus suggesting that O$_2$ release played a critical role in the ignition mechanism. This also suggests the role of gas phase oxygen towards ignition of Al–CuO and Al–Fe$_2$O$_3$ nanothermites.

Bazyn et al. [26] studied the ignition temperature and burn time of Al–MoO$_3$ and Al–Fe$_2$O$_3$ at high heating rates ($\sim10^6$ K/s) using a shock tube. They found evidence for ignition of both materials at 1400 K and 1800 K respectively. It is important to note that these temperatures are significantly higher than the melting temperature of aluminum. The findings of ignition temperatures well above the melting temperature of aluminum, and the fact that ignition temperature depends on oxidizer type, indicate that the oxidizer must play some role in the ignition mechanism at high heating rates. The thermal response of a metal oxide to heating depends on the

particular oxidizer: some materials can melt, others decompose into sub-oxides prior to melting, some can even sublimate. It has recently been shown [21] by in situ high heating rate electron microscopy ($\sim10^6$ K/s) that Al–WO$_3$ nanothermites can react via condensed phase reactions. In a separate study [27], we have used high speed X-ray phase contrast imaging to suggest that reactive sintering may be essential in the initiation of nanothermite reactions. Reactive sintering involves the exothermic release of energy that promotes reaction between two condensed phase species and leads to the formation of product particles with larger characteristic structures than the reactant particles. These larger structures result from the melting and coalescence caused by the exothermicity of the reaction and has been shown to occur very early during the reaction process (approximately within 25–50 µs after ignition). Furthermore, electron microscopy indicated the importance of reactive sintering through observation of a contact surface between nanoaluminum and the oxidizer, suggesting the existence of a solid–solid/liquid reaction. This mechanism is to be contrasted with the very different conceptual mechanism whereby nanoaluminum reacts with gas phase oxygen liberated by heating the oxidizer [23]. The reactive sintering mechanism implies that oxygen ion transport within the oxidizer should play an important role in the ignition/reaction of nanothermites. So the central question this paper seeks to answer is whether gas phase oxygen is an essential prerequisite to ignition of nanothermite. We will choose a wide range of oxidizers which release oxygen at a widely different range of temperatures, and measure the ignition temperature to verify if gas phase oxygen is necessary for the initiation of nanothermite reactions.

## 2. Experimental

### 2.1. Materials

Commercially available n-Al (Argonide Corp.) was used for all the experiments. The nominal size of the particles as specified by the supplier is $\sim$50 nm, and was determined to be 70% active using thermogravimetric analysis (TGA). The various materials and the relative size of the primary particles as specified by the manufacturers are given below in Table 1.

For the oxygen release experiments, approximately 10–15 mg of the bare oxidizers were dispersed in hexane, sonicated for 10 min and then heated as described in the experimental approach section below. Additionally, appropriate amounts of n-Al and various oxidizers listed in Table 1 are weighed to make stoichiometric sample, and then dispersed in hexane. The mixture is then sonicated for 25 min before being subjected to ignition tests.

### 2.2. Temperature-jump rapid heating experiments

To understand the importance of gas phase oxygen, a series of experiments are conducted on rapidly heated fine wires in which the optical emission and vapor phase species can be temporally monitored along with the wire temperature. These experiments are designed to extract the correlation between the oxygen release temperature from the oxidizer, if any, and the ignition temperature for the corresponding nanothermite. A thin platinum wire (length $\sim$ 12 mm, diameter $\sim$ 76 µm) is joule-heated by a tunable voltage pulse generated by a custom built power source. The transient current passing through the circuit is measured by a current probe. A small portion of the central region of the wire ($\sim$3–4 mm) is coated with the samples by pipeting a dispersion of the samples in hexane onto the wire, then allowing the hexane to evaporate. The amount of material coating the wire is estimated to be around 90 µg. From the recorded voltage and current data, the temperature of the wire at the point of ignition can be calculated from

**Table 1**
Fuel and oxidizers, source and primary particle size.

| Material | Supplier | Particle size (nm) |
|---|---|---|
| Nano-aluminum (ALEX) | Argonide Corp. | ~50 |
| Copper oxide (CuO) | Sigma–Aldrich | <50 |
| Iron oxide (Fe$_2$O$_3$) | Sigma–Aldrich | <50 |
| Tungsten oxide (WO$_3$) | Sigma–Aldrich | <50 |
| Bismuth oxide (Bi$_2$O$_3$) | Sigma–Aldrich | <50 |
| Silver iodate (AgIO$_3$) | NSW–China Lake | ~236 |
| Potassium Perchlorate (KClO$_4$) | Aerosol synthesized in our lab | ~300 |
| Tin (IV) oxide (SnO$_2$) | Sigma–Aldrich | <50 |
| Cobalt(II, III) oxide (Co$_3$O$_4$) | Sigma–Aldrich | <50 |
| Molybdenum oxide (MoO$_3$) | US Research Nanomaterials | 13–80 |
| Antimony (III) oxide (Sb$_2$O$_3$) | US Research Nanomaterials | 80–200 |

the resistivity of the wire using the well-known Callender–Van Dusen equation [28]. The resistance of the platinum wire was calibrated against a NIST calibrated blackbody source (Mikron M350) based on two color pyrometry centered on 970 nm and 1550 nm for high temperature measurement. An extrapolation of the calibration up to 1700 K was done based on Sakuma Hattori equation [29]. The maximum uncertainty associated with the determination of temperature is approximately ±50 K. Heating rate is defined as the ratio of the difference in maximum temperature and initial temperature to the pulse duration. For each test, a new wire is used since reacted material may adhere to the wire and change the electrical properties, thus presenting uncertainty in the temperature calculation. Two different sets of experiments described below are conducted to correlate the gas release to ignition.

### 2.2.1. Oxygen/gas release experiments

For the gas release experiments, the bare oxidizers are coated on the platinum wire, and heated in a customized T-Jump TOF mass spectrometer [25]. These experiments are conducted to measure the temperature of O$_2$ release from the individual oxidizers under rapid heating. The temperature of the wire corresponding to the start of the release is taken to be the temperature of oxygen release. The temporal uncertainty in the experiment is limited by the mass spectrometer which is operated at 10 kHz, corresponding to a sample every 100 μs. This translates to a wire temperature uncertainty of ~50 K assuming a maximum heating rate of ~5 × 10$^5$ K/s, and turn out also to be roughly the uncertainty in the measurement of the wire temperature. The average delay in detection of the gas species is their transit time through the time

of flight tube and is estimated to be ~10 μs which is negligible when compared to the sampling time of 100 μs. A detailed description including operational principles of the TOFMS could be found in reference [25].

### 2.2.2. Ignition experiments

To measure the ignition temperature, a separate set of experiments are carried out by coating the platinum wire with the prepared stoichiometric nanothermite samples. For these experiments, the T-Jump TOFMS system was modified by adding a photomultiplier tube (PMT), thus allowing for simultaneous collection of the mass spectra and the optical emission. The optical emission is monitored using a photomultiplier tube (PMT), and the ignition temperature is taken as the wire temperature corresponding to the onset of optical emission above the background emission from the heated wire. This allows for a direct comparison between the optical emission, commonly used as a measurement of ignition, and the time-resolved species evolved during the reaction.

## 3. Thermochemical behavior of oxidizers on heating

Before discussing the results, we first consider what happens when the individual oxidizers are heated. Certain oxidizers melt directly to the liquid phase, whereas other oxidizers decompose first to form a sub-oxide, which then melts and decomposes upon further heating. Some of the thermodynamically predicted phase changes or decompositions are calculated using the NASA-CEA software [30]. These calculations were performed at constant temperature and pressure. The pressure is fixed at 5 × 10$^{-9}$ atmosphere, which is characteristic of the pressure in the mass spectrometer chamber. Starting at around 600 K, successive calculations were performed in increments of 50 K in temperature until decomposition is observed. Phase change/decomposition data from other sources are listed for oxides which are not included in the species library of the CEA software. A summary of the behavior of the various oxides are shown below in Table 2.

It is clear from Table 2 that under the conditions of our experiments, CuO and Fe$_2$O$_3$ would decompose into respective sub-oxides Cu$_2$O (s) and Fe$_3$O$_4$ (s), releasing oxygen, before decomposing to the zero-valent metal at higher temperatures. WO$_3$ and SnO$_2$ on the other hand directly decompose into products which are all in the gas phase. The behavior of SnO$_2$ is somewhat similar to that of CuO and Fe$_2$O$_3$ as it decomposes into a sub-oxide, SnO (g) and O$_2$ (g).

AgIO$_3$ on heating decomposes into AgI (s) and O$_2$ (g) [31]. AgI (s) then undergoes melting at 831 K. Cobalt (II, III) oxide (Co$_3$O$_4$)

**Table 2**
Summary of the expected behavior of oxidizers under heating. The parentheses indicate the phase(s) of the product(s).

| Oxidizer | Temperature (K) | Event | Products | Temperature (K) | Event | Main product (s) |
|---|---|---|---|---|---|---|
| CuO | ~800[a] | Decomposes | Cu$_2$O (s), O$_2$ (g) | 1100[a] | Decomposes | Cu (s), O$_2$ (g) |
| Fe$_2$O$_3$ | ~1100[a] | Decomposes | Fe$_3$O$_4$ (s), O$_2$ (g) | 1500[a] | Decomposes | Fe (s), O$_2$ (g) |
| WO$_3$ | 1200[a] | Decomposes | (WO$_3$)$_2$ (g) (WO$_3$)$_3$ (g), etc. | – | – | – |
| SnO$_2$ | 1175[a] | Decomposes | SnO (g), O$_2$ (g) | – | – | – |
| AgIO$_3$ | 678[b] | Decomposes | AgI (s), O$_2$ (g) | 831[c] | Melts | AgI (l) |
| Co$_3$O$_4$ | 1173[c] | Decomposes | CoO (s), O$_2$ (g) | 2103[c] | Melts | CoO (l) |
| KClO$_4$ | 865[d] | Decomposes | KCl (s)[d] O$_2$ (g)[d] | – | – | – |
| MoO$_3$ | 1075[c] | Melts | MoO$_3$ (l) | 1428[c] | Boils | MoO$_3$ (g) |
| Bi$_2$O$_3$ | 1098[e] | Melts | Bi$_2$O$_3$ (l) | – | – | – |
| Sb$_2$O$_3$ | 929[c,e] | Melts | Sb$_2$O$_3$ (l) | 1703[c], 1823[e] | Vaporize | Sb$_2$O$_3$ (g) |

[a] Constant T, P calculations in CEA [30].
[b] Ref. [31].
[c] Ref. [30].
[d] Ref. [33].
[e] Ref. [34].

decomposes around 1173 K into CoO (s) and $O_2$ (g). The decomposition product CoO (s) is comparatively stable and does not melt until 2103 K [32]. $KClO_4$ is known to decompose into its potassium chloride (KCl) and $O_2$ (g) at 865 K [33]. $MoO_3$ melts at 1075 K to $MoO_3$ (l) and boils at 1428 K [32].

Alternatively, oxidizers such as $Bi_2O_3$ and $Sb_2O_3$ melt first. Not much is known about the behavior of $Bi_2O_3$ above its melting point at 1098 K [34]. On the other hand, antimony (III) oxide ($Sb_2O_3$) melts around 929 K [32,34], and then vaporizes without decomposition producing $Sb_2O_3$ (g) at 1703 K according to reference [32] and at 1823 K according to reference [34].

It is important to note that decomposition products/routes mentioned in Table 2 are based on equilibrium calculation, while the phenomenology being evaluated are very far from equilibrium conditions. Thus mass-transfer constraints within the reactive components may lead to very different results in terms of species partitioning. In addition, since our experiment is only measuring oxygen release we have no a priori knowledge as to the phase of the metal oxide. For example, our experiment cannot distinguish oxygen release from CuO leading to Cu or $Cu_2O$. Consequently, the mechanism of the reduction of the oxide under heating is of minimal interest to us and the constancy of the temperature of oxygen release from the oxidizer irrespective of the presence of aluminum is a key assumption in this work.

Before proceeding to discuss the results, it is worth mentioning that melting temperatures are generally not highly sensitive to the surrounding atmosphere or pressure. On the other hand, the decomposition temperature is nominally quoted under equilibrium conditions. The decomposition temperature of the oxidizer into a gas, based on an equilibrium calculation, is computed under a constraint of the equilibrium mole fraction of the gas phase product of the solid. Thus increasing the total system pressure also increases the decomposition temperature, so that the sum of the partial pressures of the decomposition products is equal to the total pressure, such that at equilibrium the leaving (from solid) and arrival rate (to solid) of species are equivalent. However the escape probability of a decomposing molecule on a surface is independent of the total pressure and only depends on temperature. As a result when one considers the initial decomposition one is operating far from equilibrium, the initial decomposition is independent of the total pressure. Thus one should consider the equilibrium calculations as a relative measure of products formed, and the temperature of their transformations.

## 4. Results and discussion

### 4.1. Oxygen release

Molecular oxygen is observed to be released from a majority of the oxidizers under heating. Figure 1 depicts a representative temporal plot for $O_2$ release from CuO during a temperature ramp of $\sim 5 \times 10^5$ K/s.

The results show that oxygen release is first observed at a temperature of $\sim 975$ K. Similar experiments on other neat metal oxides enable us to determine the primary evolving gas phase species and their threshold decomposition temperatures.

The temperatures of $O_2$ gas release from bare oxidizers are presented in Table 3. Most of the oxidizers release $O_2$ (except for $Bi_2O_3$ which, in addition to $O_2$, generates Bi gas) while some oxidizers do not. CuO, $Fe_2O_3$, $Bi_2O_3$, $KClO_4$, $AgIO_3$, $SnO_2$ and $Co_3O_4$ release oxygen on decomposition which has been detected by the mass spectrometer. $AgIO_3$ has the lowest oxygen release temperature at $\sim 900$ K, while $SnO_2$ exhibits the highest temperature of 1680 K. No gaseous species were detected for $MoO_3$ and $Sb_2O_3$ when the neat oxidizers are heated.
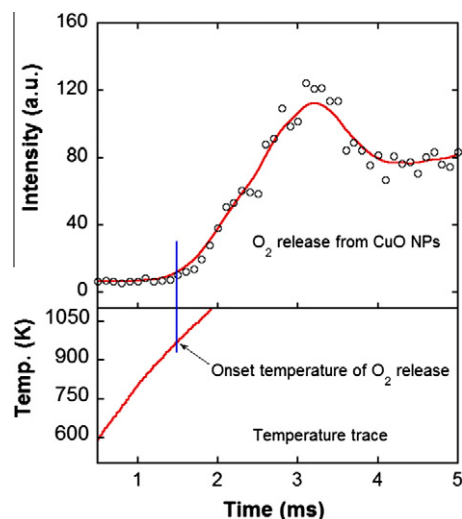


Fig. 1. Representative plot showing the temporal release of molecular oxygen from CuO when heated at $\sim 5 \times 10^5$ K/s.

Table 3

Ignition temperature of various n-Al based nanothermites listed in terms of the oxidizer. The oxygen release temperature from the nanothermite reactions and the bare oxidizer as detected by TOFMS is also tabulated. Heating rate $\sim 5 \times 10^5$ K/s.

| Nanothermite (Al + oxidizer) | Ignition temperature (K) (±50 K) | $O_2$ release temperature in thermite (K) (±50 K) | $O_2$ release from bare oxidizer (K) (±50 K) |
|---|---|---|---|
| $AgIO_3$ | 890 | 880 | 890 |
| $KClO_4$ | 905 | 905 | 875 |
| CuO | 1040 | 1050 | 975 |
| $Fe_2O_3$ | 1410 | 1400 | 1340 |
| $Co_3O_4$ | 1370 | 1020 | 1030 |
| $Bi_2O_3$ | 850 | 930 | 1620 |
| $Sb_2O_3$ | 950 | – | – |
| $MoO_3$ | 850 | – | – |
| $WO_3$ | 1030 | – | – |
| $SnO_2$ | 1050 | MS shutdown | 1680 |

The oxygen release temperature for an oxidizer is unique and specific. A reasonable presumption is that the nearby presence of aluminum oxide coated aluminum does not influence the release of $O_2$ from the metal oxide. This presents us with the opportunity to use ignition data for various nanothermite mixtures to gain an understanding of the effect of gas phase oxygen on the ignition/reaction of the corresponding nanothermite. If gas phase oxygen is essential for ignition initiation/combustion, then one would expect ignition temperature to closely track the oxygen release temperature.

### 4.2. T-Jump ignition temperatures

The temporal oxygen and aluminum signal as detected by TOF-MS during the reaction of Al–CuO nanothermite is shown in Fig. 2 (top) while the optical emission is shown below. Ignition as identified by broadband optical emission occurs $\sim 1040$ K, and is close to the temperature at which oxygen is released from the bare oxidizer (975 K), within the experimental uncertainty of ±50 K for both measurements. The optical signal is also observed to be correlated with the appearance of both the aluminum and oxygen species in this case. This is in agreement with what has been reported before in Ref. [23]. This raises an important question as to whether the release of oxygen gas is an essential precondition to ignition. To explore this hypothesis, we compare the release of oxygen from
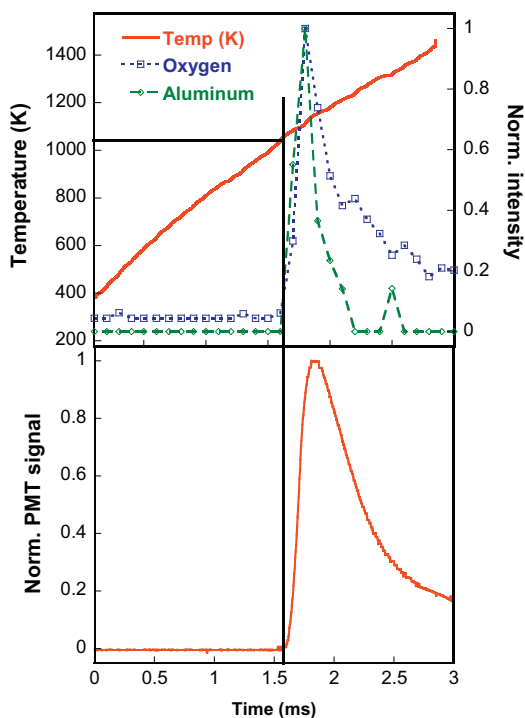
**Fig. 2.** (Top) Temporal profile of aluminum and oxygen species during the reaction of Al–CuO nanothermite mixture of stoichiometric composition. (Bottom) Optical emission showing ignition as recorded by a PMT simultaneously. The ignition temperature is the temperature of the wire corresponding to the start of optical emission as shown above and is about 1050 K for this experiment.

neat oxidizers and the corresponding ignition temperature when used as an oxidizer for aluminum in the thermite mixture. The experimental conditions i.e. total pressure in the mass spectrometer chamber, for the ignition experiments are the same as that of the gas release experiments.

The results of this comparison is shown in Table 3, which presents the observed ignition temperature, the temperature at which oxygen is detected during the nanothermite reactions, and the temperature where $O_2$ release from the neat oxidizer is also seen.

We now analyze the ignition temperature data in the context of our original motivation to determine if gas phase oxygen is
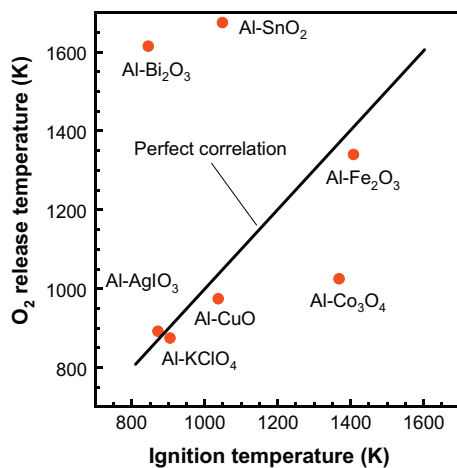


**Fig. 3.** Oxygen release temperature from neat oxide vs. ignition temperature for various n-Al based nanothermites. The straight line indicates a perfect correlation. Nanothermites of oxidizers that do not release any oxygen are not shown.

essential for ignition. Figure 3 plots the observed oxygen release temperature from the neat oxide against the observed ignition temperature.

It is evident from Fig. 3 above that there exists a good correlation between oxygen release from the oxidizer and ignition for Al–CuO, Al–Fe$_2$O$_3$, Al–AgIO$_3$ and Al–KClO$_4$ nanothermites as they lie close to the diagonal line. For these nanothermites, we find that the ignition temperature from the nanothermites and the oxygen release temperature from the bare oxidizer are the same within experimental uncertainty. However, Bi$_2$O$_3$ and SnO$_2$ nanothermites ignite (850 K and 1050 K respectively) much below their oxygen release temperatures (1620 and 1680 K). Co$_3$O$_4$ nanothermite on the other hand, is seen to ignite after oxygen release. Furthermore, it is also clear from Table 3 that the nanothermite samples made from WO$_3$, MoO$_3$ and Sb$_2$O$_3$ oxidizers ignite even though we observe no oxygen release at all. These results suggest that at least in part some of these systems may rely on a heterogeneous-condensed state reaction process. Most striking is the Al–Bi$_2$O$_3$ case where oxygen is released at 930 K during the nanothermite reaction, almost 700 K lower than the temperature when neat Bi$_2$O$_3$ releases oxygen. In this case it is likely that the exothermicity of the thermite reaction drives $O_2$ out of Bi$_2$O$_3$ independent of wire heating once ignition has occurred. It may also be noted that the Al–Bi$_2$O$_3$ and Al–MoO$_3$ are also the nanothermites which react slightly below the melting point of aluminum supporting the idea that oxygen transport in condensed phases may be driving these reactions. Due to the generation of intense ion peaks associated with ignition, the mass spectrometer system was shut down during the Al–SnO$_2$ reaction. Consequently, only the ignition data is available for this reaction. Since none of the oxidizers from the list of WO$_3$, MoO$_3$ and Sb$_2$O$_3$ release any gas, we must conclude that these are initiated by some type of condensed phase reaction [21,27]. To eliminate the possibility of aluminum vapor initiating the reaction we note that in a prior work we have shown that metal oxides appear to react in an analogous manner with carbon, which is a nonvolatile fuel [35].

Clearly then the oxygen release and ignition temperature data reported in this study indicate unambigouly that gas phase oxygen is not a generically essential species for ignition, although it might be for some specific thermite systems. *This is in fact the major result of this work.* The reader should keep in mind that even in those cases where correlation exists between $O_2$ release and ignition, causality cannot be confirmed from these experiments.

If gas-phase oxygen is not necessary for ignition for some nanothermite formulations and we presume to be left with a condensed state reaction, this still requires some type of movement, presumably by some type of diffusion. In our previous work we have postulated the importance of reactive sintering. In this mechanism interfacial reaction during heating can result in an increased mobility, and the bulk wetting of co-reactants and coarsening (sintering) of the particles into larger structures. Although commonly believed, it is actually not necessary for a particle to reach its melting temperature in order to sinter. Partial sintering can commence at the "Tammann" temperature. At this temperature, the atoms or ions in the bulk of the solid become sufficiently mobile to migrate to the surface, thus allowing them to initiate sintering. The Tammann temperature is usually taken to be $0.5T_m$ [36], where $T_m$ is the melting temperature. Using the available literature values for melting or decomposition temperature of the oxidizer we find that the computed Tammann temperature is always below the ignition temperature of the corresponding thermite. Thus it is quite reasonable to assume that reactive sintering at least commences, during the initiation process. In addition, we also must point out that reactive sintering is not only observed in nanothermites which ignite before oxygen release or without oxygen release, but is also observed in those nanothermite reactions with oxygen release. This

suggests that reaction sintering is an important component in these nanothermite systems that release oxygen prior to ignition.

## 5. Conclusions

In this study we have postulated the question if gas phase oxygen is an essential prerequisite to the initiation of nanothermite reactions by comparing the oxygen/gas release (if any) temperature with the ignition temperature for a variety of nanothermites.

Several nanothermites tested did not support the hypothesis requiring gas phase oxygen as a requirement for initiation of the nanothermite reactions. Among them, Al–$Bi_2O_3$ and Al–$SnO_2$ ignited below the oxygen release temperature from the corresponding oxidizers, while Al–$Co_3O_4$ ignited above its oxygen release temperature. Al–$MoO_3$, Al–$Sb_2O_3$ and Al–$WO_3$, where the oxidizers did not release any oxygen/gas, were seen to ignite as well showing that oxygen/gas release cannot be the sole deciding factor towards initiation of these reactions. We conclude that the initiation of nanothermite that ignite before oxygen release or without oxygen release is likely a result of direct interfacial contact between fuel and oxidizer, leading to condensed state mobility of reactive species. Thus in answer to question posed in the title "Is Gas Phase Oxygen Generation from the Oxygen Carrier an Essential Prerequisite to Ignition?", the answer is it might be in some cases, but certainly there are cases where it is not essential.

## Acknowledgments

## References

[1] M.C. Fischer, S.H. Grubelich, in: 24th International Pyrotechnics Seminar, Monterey, California, USA, 1998.
[2] B.S. Bockmon, M.L. Pantoya, S.F. Son, B.W. Asay, J.T. Mang, J. Appl. Phys. 98 (6) (2005) 064903.3.
[3] E.M. Hunt, M.L. Pantoya, J. Appl. Phys. 98 (3) (2005) 034909.
[4] G. Young, K. Sullivan, M.R. Zachariah, K. Yu, Combust. Flame 156 (2) (2009) 322–333.
[5] B.A. Mason, K.Y. Cho, C.D. Yarrington, S.F. Son, J. Gesner, R.A. Yetter, B.W. Asay, in: Silicon-Based Nanoenergetic Composites, Proceedings of the 6th Combustion Meeting, Chicago, IL, USA, 2009.
[6] K. Sullivan, M.R. Zachariah, J. Propul. Power 26 (3) (2010) 467–472.
[7] S.M. Umbrajkar, M. Schoenitz, E.L. Dreizin, Thermochim. Acta 451 (1–2) (2006) 34–43.
[8] J.J. Granier, M.L. Pantoya, Combust. Flame 138 (4) (2004) 373–383.
[9] K. Moore, M.L. Pantoya, S.F. Son, J. Propul. Power 23 (1) (2007) 181–185.
[10] M.L. Pantoya, J.J. Granier, J. Therm. Anal. Calorim. 85 (1) (2006) 37–43.
[11] V.E. Sanders, B.W. Asay, T.J. Foley, B.C. Tappan, A.N. Pacheco, S.F. Son, J. Propul. Power 23 (4) (2007) 707–714.
[12] M. Schoenitz, S. Umbrajkar, E.L. Dreizin, J. Propul. Power 23 (4) (2007) 683–687.
[13] S.F. Son, B.W. Asay, T.J. Foley, R.A. Yetter, M.H. Wu, G.A. Risha, J. Propul. Power 23 (4) (2007) 715–721.
[14] J.A. Puszynski, C.J. Bulian, J.J. Swiatkiewicz, J. Propul. Power 23 (4) (2007) 698–706.
[15] D.A. Kaplowitz, R.J. Jouet, M.R. Zachariah, J. Cryst. Growth 312 (24) (2010) 3625–3630.
[16] S. Apperson, R.V. Shende, S. Subramanian, D. Tappmeyer, S. Gangopadhyay, Z. Chen, K. Gangopadhyay, P. Redner, S. Nicholich, D. Kapoor, Appl. Phys. Lett. 91 (24) (2007) 243109.
[17] M.A. Trunov, M. Schoenitz, X.Y. Zhu, E.L. Dreizin, Combust. Flame 140 (4) (2005) 310–318.
[18] A. Rai, K. Park, L. Zhou, M.R. Zachariah, Combust. Theor. Model. 10 (5) (2006) 843–859.
[19] R. Nakamura, D. Tokozakura, H. Nakajima, J.G. Lee, H. Mori, J. Appl. Phys. 101 (7) (2007) 074303.
[20] S. Chowdhury, K. Sullivan, N. Piekiel, L. Zhou, M.R. Zachariah, J. Phys. Chem. C 114 (20) (2010) 9191–9195.
[21] K.T. Sullivan, W.A. Chiou, R. Fiore, M.R. Zachariah, Appl. Phys. Lett. 97 (13) (2010) 133104.
[22] V.I. Levitas, B.W. Asay, S.F. Son, M. Pantoya, Appl. Phys. Lett. 89 (7) (2006) 231930.
[23] L. Zhou, N. Piekiel, S. Chowdhury, M.R. Zachariah, J. Phys. Chem. C 114 (33) (2010) 14269–14275.
[24] G.Q. Jian, N. Piekiel, M.R. Zachariah, submitted for publication, J. Phys. Chem.
[25] L. Zhou, N. Piekiel, S. Chowdhury, M.R. Zachariah, Rapid Commun. Mass Spectrom. 23 (1) (2009) 194–202.
[26] T. Bazyn, N. Glumac, H. Krier, T.S. Ward, M. Schoenitz, E.L. Dreizin, Combust. Sci. Technol. 179 (3) (2007) 457–476.
[27] K. Sullivan, N. Piekiel, C. Wu, S. Chowdhury, S.T. Kelly, T.C. Hufnagel, K. Fezzaa, M.R. Zachariah, Combust. Flame 159 (1) (2012) 2–15.
[28] P.R.N. Childs, Practical Temperature Measurement, Butterworth-Heineman, 2001.
[29] P. Saunders, D.R. White, Metrologia 40 (4) (2003) 195–203.
[30] S. Gordon, B.J. McBride, in: NASA RP-1311, Washington, DC, USA, 1994.
[31] K.H. Stern, High Temperature Properties and Thermal Decomposition of Inorganic Salts with Oxyanions, CRC Press, Boca Raton, Florida, USA, 2000.
[32] W.M. Haynes, Handbook of Chemistry and Physics, CRC, 2011–2012.
[33] S.M. Pourmortazavi, M. Fathollahi, S.S. Hajimirsadeghi, S.G. Hosseini, Thermochim. Acta 443 (1) (2006) 129–131.
[34] ICT Database of Thermochemical Values Version 3.0, 2001.
[35] N. Piekiel, K. Sullivan, G. Egan, M.R. Zachariah, accepted for publication, J. Phys. Chem C, (2012), http://dx.doi.org/10.1021/jp304148c
[36] C.N. Satterfield, Heterogeneous Catalysis in Industrial Practice, 1991.